JBC RESEARCH ARTICLE

Molecular mechanisms of centipede toxin SsTx-4 inhibition of inwardly rectifying potassium channels

Received for publication, May 6, 2021, and in revised form, August 5, 2021 Published, Papers in Press, August 12, 2021,
https://doi.org/10.1016/j.jbc.2021.101076

Dongfang Tang[1,2,‡], Jiahui Xu[1,‡], Yinping Li[1], Piao Zhao[1], Xiangjin Kong[1], Haoliang Hu[1], Songping Liang[1], Cheng Tang[1,*], and Zhonghua Liu[1,*]

From the [1]The National and Local Joint Engineering Laboratory of Animal Peptide Drug Development, College of Life Sciences, Hunan Normal University, Changsha, China; [2]College of Chemistry and Bioengineering, Hunan University of Science and Engineering, Yongzhou, Hunan, China

Edited by Mike Shipston

Inwardly rectifying potassium channels (Kirs) are important drug targets, with antagonists for the Kir1.1, Kir4.1, and pancreatic Kir6.2/SUR1 channels being potential drug candidates for treating hypertension, depression, and diabetes, respectively. However, few peptide toxins acting on Kirs are identified and their interacting mechanisms remain largely elusive yet. Herein, we showed that the centipede toxin SsTx-4 potently inhibited the Kir1.1, Kir4.1, and Kir6.2/SUR1 channels with nanomolar to submicromolar affinities and intensively studied the molecular bases for toxin–channel interactions using patch-clamp analysis and site-directed mutations. Other Kirs including Kir2.1 to 2.4, Kir4.2, and Kir7.1 were resistant to SsTx-4 treatment. Moreover, SsTx-4 inhibited the inward and outward currents of Kirs with different potencies, possibly caused by a K^+ "knock-off" effect, suggesting the toxin functions as an out pore blocker physically occluding the K^+-conducting pathway. This conclusion was further supported by a mutation analysis showing that M137 located in the outer vestibule of the Kir6.2/ΔC26 channel was the key residue mediating interaction with SsTx-4. On the other hand, the molecular determinants within SsTx-4 for binding these Kir channels only partially overlapped, with K13 and F44 being the common key residues. Most importantly, K11A, P15A, and Y16A mutant toxins showed improved affinity and/or selectivity toward Kir6.2, while R12A mutant toxin had increased affinity for Kir4.1. To our knowledge, SsTx-4 is the first characterized peptide toxin with Kir4.1 inhibitory activity. This study provides useful insights for engineering a Kir6.2/SUR1 channel–specific antagonist based on the SsTx-4 template molecule and may be useful in developing new antidiabetic drugs.

As an important subset of the potassium channel superfamily, the inwardly rectifying potassium channels (Kirs) are characterized by conducting inwardly rectifying K^+ flow across the cell membrane (1). The core structure of Kir channels is constructed by a fourfold-symmetric assembling of four pore-forming Kir subunits (2). In mammals, 15 Kir subunits are identified, which can form four different groups of Kir channels: the K^+ transport channels (Kir1.1, Kir4.1–4.2, Kir5.1, and Kir7.1), the classical Kir channels (Kir2.1–2.4), the G-protein–gated K_G channels (Kir3.1–3.4), and the ATP-sensitive K_{ATP} channels (Kir6.1–6.2) (2, 3). Each Kir subunit is composed of two transmembrane segments (M1 and M2 helix), a reentrant M1–2 linker, and the intracellular N and C termini (2). The K^+-conducting pore in Kir channel can be artificially divided into three parts, with the turret loop, as well as the sequence between the selectivity filter (SF) and M2 helix constructing the outer vestibule, the signature sequence "T-X-G-Y(F)-G" in the M1–2 linker highly conserved across the K^+ channel superfamily serving as the SF, and the M2 helix mainly forming the central cavity (4, 5). Among these Kir channels, the K_{ATP} channels are unique as they are octamers made by a close association of four additional sulfonylurea receptor (SUR) subunits with the four core pore-forming Kir6.x subunits, in which SURs surround and gate of the pore (6, 7). Up to date, three different SUR proteins are identified (SUR1, SUR2A, and SUR2B) (8–10). The molecular constituents of different K_{ATP} channels are varied depending on their tissue distributions, with Kir6.2+SUR1, Kir6.2+SUR2A, and Kir6.1+SUR2B being the combinations in pancreatic beta cells, cardiac cells, and smooth muscle cells, respectively (11–14).

The inwardly rectifying characteristic in Kir channels is caused by blockade of the channel pore by intracellular cations such as Mg^{2+} and polyamines at voltages positive than the equilibrium potential of K^+(E_K) (15, 16). However, the blockade is incomplete and the channel would conduct outward K^+ currents to repolarize the cell membrane in this condition. Accordingly, the key function of Kir channels is regulating K^+ homeostasis and maintaining the resting membrane potential (E_{res}), thereby they play critical physiological and pathophysiological roles (2). In the kidney, Kir1.1 and the Kir4.1/5.1 heteromeric channels are expressed in thick ascending limb of Henle (TALH), distal convoluted tubule (DCT), and cortical collecting ducts (CCD) regions, cooperating with transporters such as Na^+-K^+-$2Cl^-$ and epithelial sodium channels to reabsorb salt (17). Homozygous loss-of-function mutation of Kir1.1 causes Bartter syndrome type II characterized by polyuria, salt wasting, and low blood pressure

‡ These authors contributed equally to this work.
* For correspondence: Cheng Tang, chengtang@hunnu.edu.cn; Zhonghua Liu, Liuzh@hunnu.edu.cn.

(18). However, heterozygous Kir1.1 loss-of-function mutation carriers are healthy and have a lower risk of suffering hypertension (19). On this basis, Kir1.1 antagonists are promising candidates for developing diuretics (17). As regard to the Kir4.1 channel, its critical role in tuning lateral habenula neuronal bursting suggests selectively blocking Kir4.1 activity might be a promising strategy for treating depression (20). The Kir6.2/SUR1 channel might be the most intensively studied Kir subtype and is a successful drug target for treating type 2 diabetes mellitus, with the clinically used type 2 diabetes mellitus drugs sulfonylureas stimulating insulin release by inhibiting its activity (21). Now, it is clarified that the Kir6.2/SUR1 channel regulates the E_{res} of pancreatic beta cells and is a key component of the insulin secretion pathway, in which its loss- or gain-of-function mutations cause hyperinsulinemia or diabetes, respectively (22–25). Moreover, its gating by intracellular ATP-ADP ratio has coupled insulin release with the metabolism state of the cell (26).

The physiological and pathological significances of these Kir channels have motivated development of their antagonists, used as either drug candidates or pharmacological tools for investigating their structures and functions (2, 27). The documented Kirs' pore-blocking antagonists fall into two groups, the small-molecule chemicals that tend to bind to the central cavity of the pore (28–31) and the hydrophilic protein inhibitors from animal venoms that prefer to act on the extracellular side of the channel by binding to the outer vestibule region (32). It is shown that the sequences in the central cavity rather than the vestibule region are highly conserved across different Kir channels. Therefore, it is more likely to develop subtype-specific Kir antagonists targeting the outer vestibule region. On the other hand, although many small chemicals targeting the Kir1.1 (17), Kir4.1 (31, 33), and Kir6.2/SUR1 (14) channels were reported, few protein inhibitors for them were identified to date. Dendrotoxin (34), TPN (35), and Lqh-2 (36) were reported to potently block the Kir1.1 channel with nanomolar affinity. The mechanism of TPN inhibiting the Kir1.1 channel was also intensively studied, and molecular engineering has generated a subtype-specific Kir1.1 antagonist, TPN_{LQ} (35, 37–39). SpTx-1 (40), SsTx, and SsdTx1-3 (41) from centipede venom are Kir6.2/SUR1 channel antagonists; however, their action mechanisms are still to be elucidated. No protein inhibitor for Kir4.1 channel was reported yet. In the present study, we have identified a peptide toxin, SsTx-4, potently inhibiting the currents of Kir1.1, Kir4.1, and Kir6.2/SUR1 channels with nanomolar to submicromolar affinities from the venom of *Scolopendra subspinipes mutilans*. SsTx-4 showed high homology to SsdTx-1-3 and SsTx (>75% sequence identity); however, the activity of SsdTx-1-3 and SsTx on Kir1.1 and Kir4.1 channels was never reported. We further explored the molecular mechanisms of SsTx-4 acting on these three Kir channels. Our data revealed that SsTx-4 blocked the out pore of Kir1.1, Kir4.1, and Kir6.2/SUR1 channels, with M137 in the outer vestibule of the Kir6.2/SUR1 channel being identified as the key residue for toxin binding. Interestingly, the molecular determinants in SsTx-4 for its interaction with the three Kir channels were only partially overlapped, allowing us to improve the toxin's selectivity and/or activity toward a given subtype by molecular engineering. As a result, the K11A, P15A, and Y16A mutant toxins showed improved affinity and/or selectivity to Kir6.2, while R12A mutant toxin had increased affinity with the Kir4.1 channel. To our knowledge, SsTx-4 is the first reported Kir4.1 protein inhibitor, and this study has paved the way for engineering the Kir6.2/SUR1 channel–specific antagonist based on SsTx-4.

Results

Purification and characterization of SsTx-4

We screened antagonists for Kir channels from our local peptide-toxin library containing hundreds of RP-HPLC purified fractions of several animal venoms, and an active component was identified in the venom of *S. subspinipes mutilans* (Fig. 1*B* and Fig. S1*A*) to effectively block the currents of the Kir6.2/SUR1 channel heterologously expressed in HEK293T cells. The subsequent activity-guided purification has purified this component to homogeneity (Fig. S1, *A–D*). The MW of this peptide toxin was determined as 6037.959 Da by electrospray ionization MS analysis (Fig. S1*E*), and its full sequence was determined by using Edman degradation sequencing and 5′-RACE. As shown in Figure 1*A*, the toxin is composed of 53 residues including four cysteines, which should form two intramolecular disulfide bonds as the theoretical MW (6042.01 Da) is 4 Da more than that observed by MS. We named this toxin as SsTx-4. Blasting its sequence in the database showed it has high homology to several centipede toxins including SsTx and SsdTx1-3 (Fig. 1*A*). SsTx and SsdTx1-3 were reported as the Kir6.2/SUR1 channel antagonists, with the NMR structure of SsTx determined in previous studies (41, 42). Therefore, it is not surprising that SsTx-4 also potently inhibited the Kir6.2/SUR1 channel, and the disulfide bond mode in SsTx-4 should be C_1–C_3 and C_2–C_4, the same as that in SsTx (Fig. 1*A*; number indicating the relative position of cysteine residues in the sequence). We referred to SsTx-4 purified from the venom as nSsTx-4 to discriminate it from the recombinantly expressed toxin (rSsTx-4) shown later. nSsTx-4 dose-dependently inhibited the Kir6.2/SUR1 currents with an IC_{50} of 42.5 ± 3.5 nM and 75.4 ± 1.9 nM, at −140 mV and −40 mV, respectively (Fig. 1, *C* and *D*). The small but significant differences between toxin's efficacy in inhibiting Kir6.2/SUR1 currents at −140 mV and −40 mV indicated it inhibited the channel voltage dependently (Fig. 1*D*). An expanded survey of nSsTx-4's activity on other Kir channels showed that it also potently inhibited the currents of Kir1.1 and Kir4.1 (Fig. 1*E*), with the IC_{50} determined as 89.2 ± 6.7 nM and 360.1 ± 75.8 nM at −140 mV, and an increased IC_{50} of 209.7 ± 16.8 nM and 6.2 ± 1.2 μM at −40 mV, for Kir1.1 and Kir4.1, respectively (Fig. 1*F*). To the best of our knowledge, SsTx-4 represented the first identified peptide antagonist of the Kir4.1 channel.

Recombinant SsTx-4 had the same activity on Kir channels as nSsTx-4

To further confirm the activity of SsTx-4, we recombinantly expressed the toxin in *E. coli* (rSsTx-4) and compared its activity

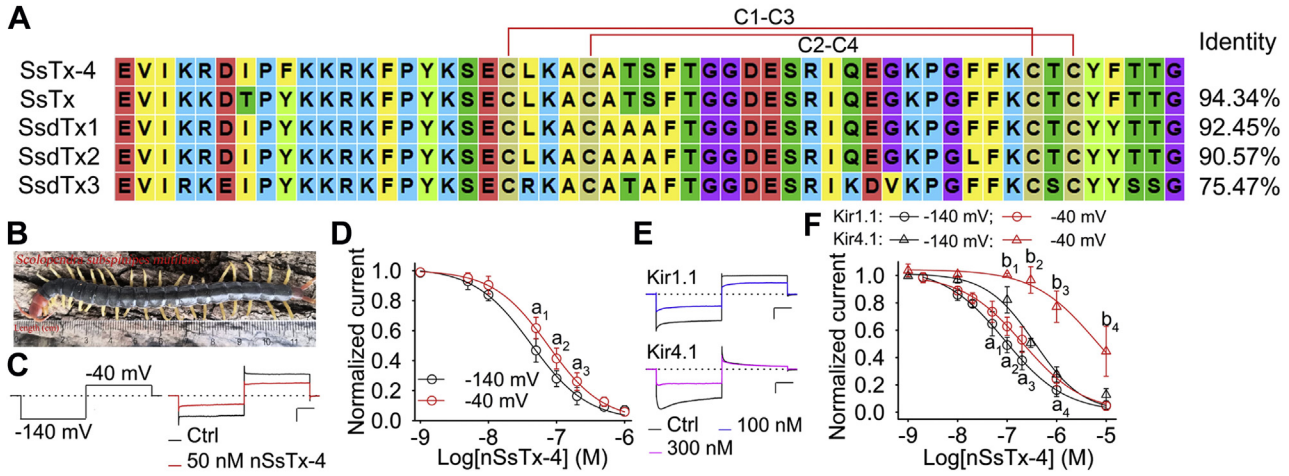

Figure 1. Characterization of SsTx-4. *A*, sequence alignment of SsTx-4 with other centipede toxins inhibiting the Kir6.2/SUR1 channel. *B*, the centipede *Scolopendra subspinipes mutilans*. *C*, representative traces showing the native SsTx-4 (nSsTx-4) potently inhibited Kir6.2/SUR1 currents; currents were elicited by the voltage protocol as shown (scale bar, 2 nA × 25 ms; n = 5). *D*, dose–response curves of nSsTx-4 inhibiting Kir6.2/SUR1 currents; the IC_{50} values were determined as 42.5 ± 3.5 nM and 75.4 ± 1.9 nM at −140 mV and −40 mV, respectively (a_1, $p = 0.0019$; a_2, $p = 0.0045$; a_3, $p = 0.0036$; when comparing the normalized I value at −140 mV with that at −40 mV, paired *t* test; n = 4–5). *E*, representative traces showing the inhibition of Kir1.1 and Kir4.1 currents by nSsTx-4; the voltage protocol is the same as in panel *C* (scale bar, 2 nA × 25 ms; n = 5–6). *F*, dose–response curves of nSsTx-4 inhibiting Kir1.1 and Kir4.1 currents, with the IC_{50} determined as 89.2 ± 6.7 nM and 209.7 ± 16.8 nM for Kir1.1 and 360.1 ± 75.8 nM and 6.2 ± 1.2 μM for Kir4.1, at −140 mV and −40 mV, respectively (a_1, $p < 0.0001$; a_2, $p = 0.0002$; a_3, $p < 0.0001$; a_4, $p = 0.0011$; b_1, $p = 0.0283$; b_2, $p = 0.001$; b_3, $p = 0.0021$; b_4, $p = 0.0196$; when comparing the normalized I value at −140 mV with that at −40 mV, paired *t* test; n = 5–6). Kirs, inwardly rectifying potassium channels.

with nSsTx-4. The toxin was expressed as a soluble fusion protein with thioredoxin (thioredoxin-6×His-EK-TEV-toxin, see Experimental procedures), and TEV protease digestion released it as a toxin monomer (Fig. 2*A*). Through a single round of RP-HPLC purification, rSsTx-4 was readily purified to homogeneity (Fig. 2*B*). The yield is approximately 1 mg/l. As TEV protease cuts at the C terminus of the glutamine residue in its recognition sequence (ENLYFQ/G), rSsTX-4 would have an additional glycine residue at its N terminus compared with nSsTx-4. Accordingly, MS analysis has determined the MW of rSsTx-4 as 6094.98 Da (Fig. S2*A*). Furthermore, we showed that this additional glycine residue at the toxin's N terminus did not affect its activity (Fig. 2*C*). At −140 mV, rSsTx-4 inhibited the currents of Kir6.2/SUR1, Kir1.1, and Kir4.1 channels with an IC_{50} 12.5 ± 1.0 nM, 35.9 ± 11.7 nM, and 646.0 ± 243.1 nM, respectively (Fig. 2, *D* and *E*; black curves). As it was observed in nSsTx-4, there was an attenuation of rSsTx's efficacy at −40 mV, with the IC_{50} at −40 mV determined as 22.5 ± 1.4 nM, 60.4 ± 6.6 nM, and 5.6 ± 0.5 μM for Kir6.2/SUR1, Kir1.1, and Kir4.1, respectively (Fig. 2, *D* and *E*; red curves). Accordingly, both nSsTx-4 and rSsTx-4 inhibited these Kirs' outward currents with less efficacy than that of their inward currents, especially for Kir4.1. Similar observations were found in the inhibition of pore-blocking toxins such as charybdotoxin on Kv channels (43). We proposed that SsTx-4 blocked the Kir channels by binding with their out vestibule regions, using a positively charged lysine residue to compete the most extracellular K^+-binding site, as that of charybdotoxin acting on K_V channels (43–45). This is contrary to the voltage-dependent "knockoff" behavior observed in small-molecule blockers occluding the inner pore of the Kir channels, in which hyperpolarization-driven inward K^+ inflow but not depolarization-driven K^+ outflow impaired blockers' effect (28, 29, 46). In addition, 2 μM rSsTx-4 did not affect the currents of Kir2.1 to 2.4, Kir4.2, and Kir7.1 channels (Fig. S2*B*). The inhibition of rSsTx-4 on these three Kir channels was reversible, the time constant for toxin dissociating from the channel (τ_{off}) was determined as 8.9 ± 0.9 s, 12.6 ± 3.8 s, and 12.6 ± 3.7 s, for Kir6.2/SUR1, Kir1.1, and Kir4.1, respectively (Fig. 2*F*).

The key molecular determinants in the Kir6.2/SUR1 channel involved in interacting with SsTx-4

We further studied the molecular mechanisms of SsTx-4 acting on these Kir channels. First, the molecular determinants in the Kir6.2/SUR1 channel for binding with SsTx-4 were explored. To eliminate the possibility of SsTx-4 inhibiting the channel by affecting the SUR1 subunit, we tested its activity on the Kir6.2/ΔC26 truncate channel, which is functionally expressed in HEK293T cells independent of SUR1 (47). As shown in Figure 3, *B* and *C*, rSsTx-4 also dose dependently inhibited the currents of the Kir6.2/ΔC26 channel with an IC_{50} of 8.2 ± 0.6 nM and 17.4 ± 2.9 nM at −140 mV and −40 mV, respectively. Similarly, the toxin showed attenuated efficacy in inhibiting the currents at −40 mV compared with that at −140 mV (Fig. 3*C*). These data demonstrated that SsTx-4 directly interacted with Kir6.2 subunit to inhibit the channel. As mentioned above, SsTx-4 might bind with Kir channel's out pore, which is formed by channel's M1–M2 extracellular loop. We used an alanine-scan strategy to identify the key amino acids in this region using Kir6.2/ΔC26 as the parental channel. Residues in the M1–2 loop, except for those in the SF and the pore helix, were mutated (Fig. 3*A*). 14 of 29 mutants were functionally expressed in HEK293T cells, and testing the activity of 1 μM rSsTx-4 on them showed that only the M137A mutation remarkably reduced toxin's potency (Fig. 3, *B* and *E*). The IC_{50} of

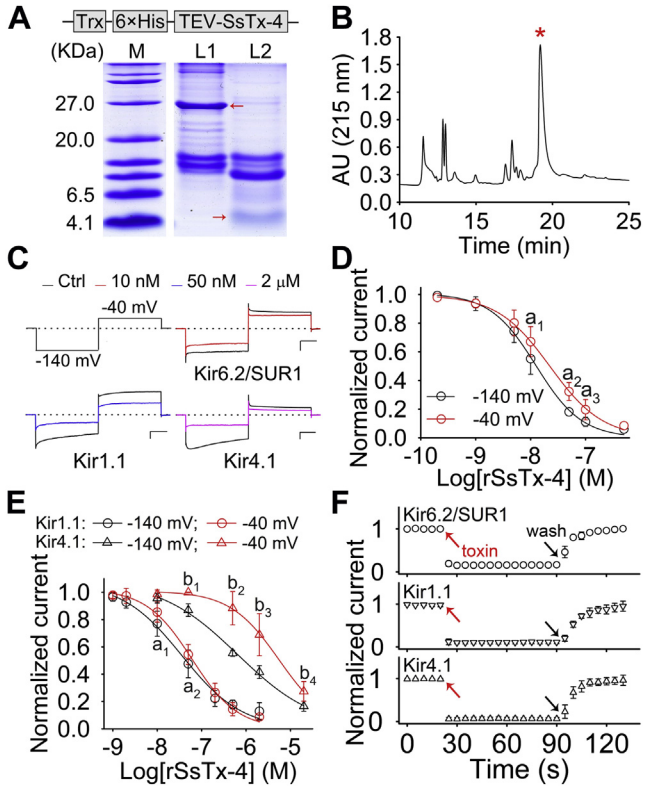

Figure 2. Activity assay of recombinant SsTx-4. *A*, *upper panel*, architecture of recombinant SsTx-4 fusion protein; *lower panel*, tricine SDS-PAGE analysis of Ni bead–purified recombinant protein before (L1) and after (L2) TEV digestion, with the *red arrows* in L1 and L2 indicating the SsTx-4 fusion protein and SsTx-4, respectively. *B*, RP-HPLC purification of the recombinant SsTx-4 (rSsTx-4); the *red star*–labeled peak indicates rSsTx-4. *C*, representative traces showing rSsTx-4 potently inhibited the currents of Kir6.2/SUR1 (n = 5), Kir1.1 (n = 8) and Kir4.1 (n = 5) channels (scale bar, 1 nA × 25 ms). Currents were elicited by the voltage protocol as shown. *D*, the dose–response curves of rSsTx-4 inhibiting Kir6.2/SUR1 channel; the IC_{50} were determined as 12.5 ± 1.0 nM and 22.5 ± 1.4 nM at −140 mV and −40 mV, respectively (a_1, $p < 0.0001$; a_2, $p < 0.0001$; a_3, $p = 0.0081$; when comparing the normalized I value at −140 mV with that at −40 mV, paired *t* test; n = 5–8). *E*, dose–response curves of rSsTx-4 inhibiting the Kir1.1 and Kir4.1 channels. The IC_{50} were determined as 35.9 ± 11.7 nM and 60.4 ± 6.6 nM for Kir1.1 and 646.0 ± 243.1 nM and 5.6 ± 0.5 μM for Kir4.1 at −140 mV and −40 mV, respectively (a_1, $p = 0.0218$; a_2, $p = 0.0275$; b_1, $p = 0.0028$; b_2, $p = 0.0034$; b_3, $p = 0.0226$; b_4, $p = 0.0091$; when comparing the normalized I value at −140 mV with that at −40 mV, paired *t* test; n = 5–8). *F*, time course of rSsTx-4 binding with and washed off the Kir6.2/SUR1, Kir1.1, and Kir4.1 channels by bath solution perfusion (the current inhibition was complete within one sweep interval of 5 s, and τ_{off} which represents the time constant of toxin dissociating from the channel was determined as 8.9 ± 0.9 s, 12.6 ± 3.8 s, and 12.6 ± 3.7 s for Kir6.2/SUR1, Kir1.1, and Kir4.1, respectively; n = 5–7). M, protein ladder marker; Kirs, inwardly rectifying potassium channels.

rSsTx-4 inhibiting the Kir6.2/ΔC26/M137A mutant channel was determined as 1.3 ± 0.2 μM and 4.9 ± 0.8 μM, at −140 mV and −40 mV, respectively (Fig. 3*D*), and an approximately 159-fold reduction of SsTx-4's affinity with the channel was observed (calculated using the IC_{50} values at −140 mV). These data further confirmed that SsTx-4 binds to the outer vestibule region of the Kir6.2/ΔC26 channel.

The key molecular determinants in SsTx-4 for binding with Kir channels

SsTx-4 has a secondary structure of βαββ, in which a P–P segment (the sequence between P8 and P15) containing several positively charged residues connects the N-terminal β sheet and its downstream α helix (Fig. 4*A*). It is shown that mutations of two positively charged residues (R11 and K15) in the P–P segment of SpTx-1 dramatically reduced toxin's activity on the $Kir6.2^{bgd}$ channel (41). We first focused on the P–P region of SsTx-4 to identify the key residues involved in interacting with the Kir6.2/ΔC26 channel. Toxins with mutated residues in or neighboring the P–P region of SsTx-4, including P8A, F9A, K10A, K11A, R12A, K13A, F14A, P15A, Y16A, and K17A, were successfully produced in *E. coli*. Testing their activity on the Kir6.2/ΔC26 channel showed that both the K13A and F14A mutations profoundly reduced toxin's potency, with an approximately 53- and 21-fold increment of the IC_{50} when compared with that of the WT SsTx-4, respectively (Fig. 4*B*, left panel). Mutating other residues in this region, including K10 which is analogous to R11 in SpTx-1, all did not remarkably reduce toxin's potency on Kir6.2/ΔC26. Conversely, the mutation Y16A in SsTx-4 caused an approximately 5-fold decrement of toxin's IC_{50} against the channel (Fig. 4*B*, left panel). The key residue K13 in SsTx-4 is analogous to the key residue K15 in SpTx-1, suggesting that they act on the Kir6.2/SUR1 channel using partially overlapped key site.

The activity of many pore-blocking K_V toxins relies on a functional dyad formed by a hydrophobic residue and a neighboring positively charged K or R residue on toxins' ββ sheet region (48, 49). In SsTx-4, K4, K40, and K45 are adjacent to Y49, forming a positively charged ring surrounding a hydrophobic center on the ββ sheet face, while F43 and F44 are neighbored by K45 and the P–P segment (Fig. 4*A*). We asked whether these residues contributed to the action of SsTx-4 on Kir6.2/ΔC26. As a result, mutating K4, K40, and K45 in SsTx-4 separately only slightly increased toxin's IC_{50} against the Kir6.2/ΔC26 channel by less than six folds (Fig. 4*B*, left panel). However, combinatorial mutations of these K residues greatly attenuated toxin's activity, as revealed by that K4/K40, K4/K45, K40/K45, and K4/K40/K45 mutations increased the IC_{50} by approximately 9, 11, 19, and 39 folds, respectively (Fig. 4*B*, left panel). As for those hydrophobic residues, F43A and F44A mutations increased toxin's IC_{50} by approximately 8 and 16 folds, respectively, and F43/F44 double mutations further increased the IC_{50} value by approximately 116 folds (Fig. 4*B*, left panel). Contrarily, Y49A mutation did not reduce but slightly increased the potency of SsTx-4 by approximately 2-folds (Fig. 4*B*, left panel). Taken together, these data suggested that the three positively charged residues K4, K40, and K45, as well as the two hydrophobic residues F43 and F44 might compensate for each other in toxin's interaction with the Kir6.2/ΔC26 channel.

The molecular determinants in SsTx-4 for interacting with the Kir1.1 are partially overlapped with that for the Kir6.2/ΔC26 channel. The P–P segment in toxin contains both the common and the unique key residue. K13A and F14A mutations profoundly increased toxin's IC_{50} against Kir1.1 by approximately 63- and 14- folds, respectively, comparable with that observed in the Kir6.2/ΔC26 channel (Fig. 4*B*, middle panel). Interestingly, the K11A mutation which did not affect

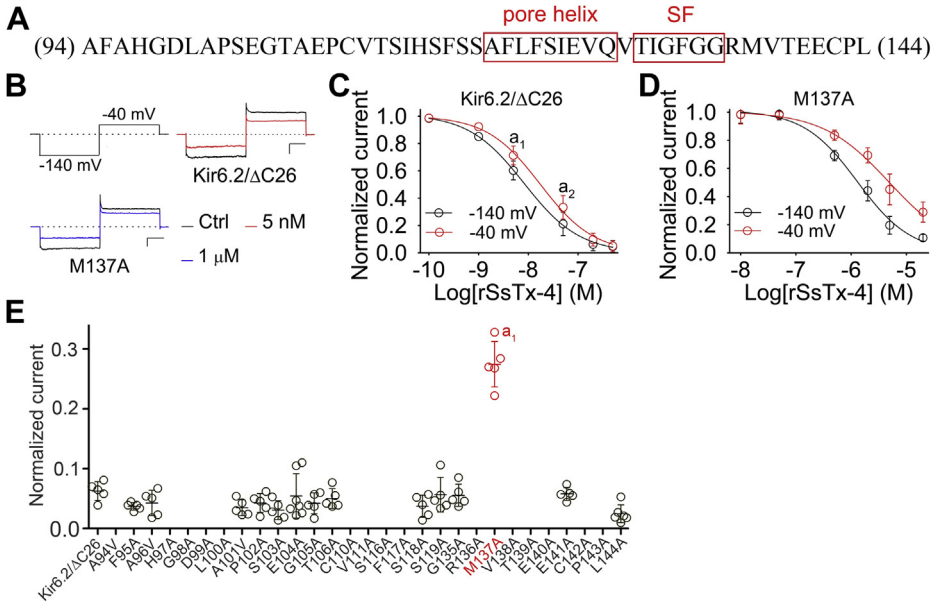

Figure 3. The key residues in the Kir6.2/SUR1 channel involved in interacting with SsTx-4. *A*, the protein sequence of M1–2 loop of Kir6.2, the pore helix, and selectivity filter (SF) regions are highlighted. *B*, representative traces showing rSsTx-4 inhibited the currents of Kir6.2/ΔC26 and M137A mutant channels with different potency; currents were elicited by the voltage protocol as shown (n = 5–6; scale bar, 1 nA × 25 ms). Note that different concentrations of toxin were used. *C* and *D*, the dose–response curves of rSsTx-4 inhibiting Kir6.2/ΔC26 (*C*) and M137A (*D*) mutant channels. The IC_{50} values were determined as 8.2 ± 0.6 nM and 17.4 ± 2.9 nM for Kir6.2/ΔC26 and 1.3 ± 0.2 μM and 4.9 ± 0.8 μM for M137A mutant channel at −140 mV and −40 mV, respectively (a_1, $p < 0.0001$; a_2, $p = 0.0041$; when comparing the normalized I value at −140 mV with that at −40 mV; paired *t* test; n = 5–6). *E*, statistics of 1 μM rSsTx-4 inhibiting Kir6.2/ΔC26 and its mutant channels as shown; each scatter plot represents the normalized I value from a separate experimental cell. Note that M137A mutation remarkably reduced toxin's inhibition on the channel (a_1, $p < 0.0001$; one-way ANOVA with post hoc analysis using the Dunnett's method; n = 5–7). Kirs, inwardly rectifying potassium channels; SUR, sulfonylurea receptor.

toxin's affinity with Kir6.2/ΔC26 greatly increased the IC_{50} against Kir1.1 channel by approximately ten folds, suggesting K11 is unique for SsTx-4 binding with Kir1.1 (Fig. 4*B*, middle panel). Other mutations including F9A and P15A only moderately reduced toxin's affinity with Kir1.1 (4- to 5-fold change of IC_{50}), while K10A, R12A, Y16A, and K17A mutations in SsTx-4 had little effect (Fig. 4*B*, middle panel). On the other hand, the residues on the ββ sheet face of SsTx-4 seemed to be less involved in interacting with Kir1.1 than that in the Kir6.2/ΔC26 channel. The F43A/F44A mutations only slightly increased toxin's IC_{50} against the Kir1.1 channel by approximately 8-folds, compared with an approximately 116-fold increment observed in the Kir6.2/ΔC26 channel (Fig. 4*B*, left and middle panels). This discrepancy is possibly caused by less contribution of F43 in toxin's binding with Kir1.1, as revealed by that F43A mutation moderately increased toxin's IC_{50} against Kir6.2/ΔC26 by 8-fold but not for Kir1.1, while F44A mutation caused a comparable reduction of toxin's affinity with both channels (approximately 11- and 16-fold change of the IC_{50} for Kir1.1 and Kir6.2/ΔC26, respectively; Fig. 4*B*, left and middle panels). K4A/K40A/K45A triple mutations in SsTx-4 significantly decreased toxin's

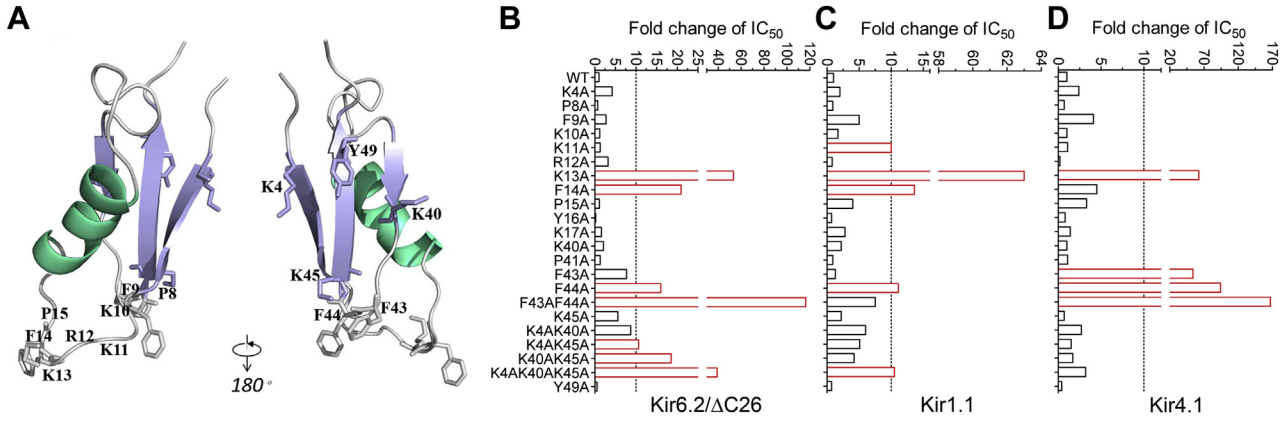

Figure 4. The key residues in SsTx-4 involved in interacting with Kir channels. *A*, the structure of SsTx-4 produced by SWISS-MODEL using SsTx as the template, residues in the P–P segment (the sequence between P8 and P15), and several residues on the ββ sheet face of the toxin are highlighted. Statistics of the fold change of IC_{50} values (mean) of each SsTx-4 mutant inhibiting the (*B*) Kir6.2/ΔC26, (*C*) Kir1.1, and (*D*) Kir4.1 channels at −140 mV, when compared with that of the WT toxin (n = 5–7). Kirs, inwardly rectifying potassium channels.

affinity with the Kir1.1 channel, but to a less extent than that in the Kir6.2/ΔC26 channel as well (approximately 11-fold *versus* 39-fold increment of IC_{50}, in Kir1.1 and Kir6.2/ΔC26, respectively; Fig. 4*B*, left and middle panels). K4A/K40A, K4A/K45A, and K40A/K45A double mutations in toxin also have less effect in Kir1.1 than that in Kir6.2/ΔC26 (Fig. 4*B*, left and middle panels).

K13, F43, and F44 in SsTx-4 were identified as the key residues for its binding with Kir4.1 as well. K13A mutation reduced toxin's affinity with Kir4.1 to a similar extent as that observed in Kir1.1 and Kir6.2/ΔC26 (approximately 62-fold change of IC_{50}; Fig. 4*B*). However, F43 and F44 in toxin likely played a much more critical role in binding with Kir4.1 than that in Kir1.1 and Kir6.2/ΔC26, as revealed by F43A and F44A mutation causing approximately 54- and 94-fold increment of toxin's IC_{50} against Kir4.1, respectively (Fig. 4*B*). Interestingly, the F14A mutation only moderately increased toxin's IC_{50} against Kir4.1 by approximately 5-folds, compared with an approximately 14- and 21-fold increment observed in Kir1.1 and Kir6.2/ΔC26, respectively (Fig. 4*B*). Mutating residues in the positively charged ring (K4A, K40A, K45A, K4A/K40A, K4A/K45A, K40A/K45A, and K4A/K40A/K45A) had little effect on toxin's potency as well (less than 5-fold increment of IC_{50}; Fig. 4*B*, right panel). On the other hand, R12A and Y49A mutations have increased toxin's affinity with Kir4.1, as revealed by an approximately 5- and 3-fold decrement of the IC_{50}, respectively (Fig. 4*B*, right panel).

Mutant toxins with improved selectivity and/or affinity to specific Kir subtypes

Normalizing the calculated IC_{50} of mutant toxins on Kir1.1 to that of Kir6.2/ΔC26 showed K11A, P15A, and Y16A mutations in SsTx-4 greatly improved its selectivity to Kir6.2/ΔC26 against Kir1.1 (Fig. 5*A*). We further determined their IC_{50} values of inhibiting Kir1.1, Kir6.2/ΔC26, and Kir4.1 channels by constructing the dose–response curves (Fig. 5, *B–D*). It is no surprise that the IC_{50} values derived from the curves were close to that determined using the single dose inhibition ratio in Figure 4. K11A and P15A mutant toxins had reduced affinity with Kir1.1 but intact affinity with Kir6.2/ΔC26, thus showing approximately 32- and 16-fold selectivity to the latter, respectively (Fig. 5, *A–C*). The Y16A mutation, however, increased toxin's affinity with Kir6.2/ΔC26 but did not affect that for Kir1.1, showing approximately 16-fold selectivity to Kir6.2/ΔC26 as well (Fig. 5, *A* and *D*). The selectivity of K11A, P15A, and Y16A to Kir6.2/ΔC26 against the Kir4.1 channel is approximately 99, 222, and 234 folds, respectively (Fig. 5, *B–D*). On the other hand, the R12A mutation in SsTx-4 increased toxin's affinity with Kir4.1, with the IC_{50} determined as 25.0 ± 0.4 nM, 39.1 ± 16.0 nM, and 122.6 ± 29.0 nM, for Kir1.1, Kir6.2/ΔC26, and Kir4.1, respectively (Fig. 5*E*). Taken together, these data suggested that even single mutation in SsTx-4 could improve toxin's affinity and/or selectivity because of varied key residues in toxin for interacting with the three Kir channels.

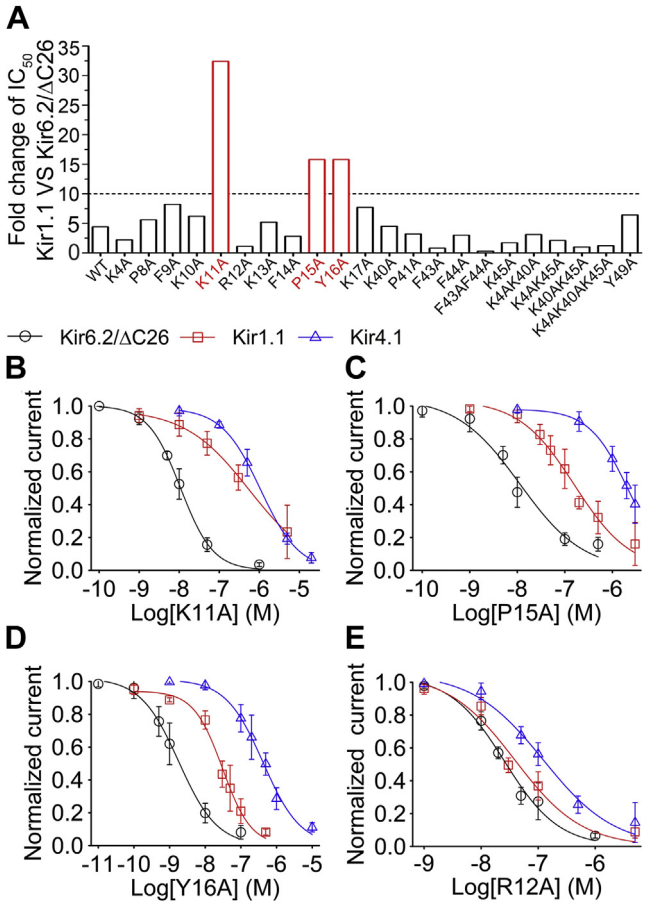

Figure 5. Mutant toxins showing improved selectivity and/or potency. *A*, statistics of the fold change of IC_{50} (mean) of each SsTx-4 mutant inhibiting the Kir1.1 channel when compared with that for the Kir6.2/ΔC26 channel (n = 5–7). Note that K11A, P15A, and Y16A mutant toxins showed improved selectivity to Kir6.2/ΔC26 against Kir1.1. *B–E*, the dose–response curves of K11A (*B*), P15A (*C*), Y16A (*D*), and R12A (*E*) mutant toxins inhibiting the Kir6.2/ΔC26 (*black*), Kir1.1 (*red*), and Kir4.1 (*blue*) channels at −140 mV. The IC_{50} values of K11A, P15A, Y16A, and R12A mutant toxins were determined as 10.8 ± 0.6 nM, 9.7 ± 5.3 nM, 1.8 ± 0.3 nM, and 25.6 ± 4.0 nM against Kir6.2/ΔC26, 561.2 ± 34.4 nM, 159.7 ± 31.0 nM, 30.4 ± 4.0 nM, and 39.1 ± 16.0 nM against Kir1.1, and 1065.1 ± 39.2 nM, 2158.2 ± 29.7 nM, 420.5 ± 53.5 nM, and 122.6 ± 29.0 nM against Kir4.1, respectively (n = 5–6). Kirs, inwardly rectifying potassium channels.

Discussion

The present study has identified the centipede toxin SsTx-4 as a novel antagonist of the Kir1.1, Kir4.1, and Kir6.2/SUR1 channels, which functioned by physically occluding the channel's K^+ conducting pathway by binding with the outer vestibule region. Moreover, mutation analysis has revealed the molecular bases for toxin–channel interactions, in which M137 in Kir6.2 was identified as the key residue for binding with SsTx-4, and the molecular determinants in toxin for interacting with the three Kir channels were only partially overlapped. Accordingly, several mutant toxins showed improved selectivity and/or affinity toward the Kir6.2/SUR1 and Kir4.1 channels. Taken together, SsTx-4 is the first identified protein inhibitor of the Kir4.1 channel, and the present study has paved the way for engineering specific Kir6.2/SUR1 channel antagonist based on SsTx-4.

Kir6.2 or SUR1 mutations that increase pancreatic Kir6.2/SUR1 currents cause permanent neonatal diabetes mellitus (PNDM) (50–52); some PNDM patients are resistant to sulfonylurea treatment because of reduced or lost inhibition of the mutant channel by drugs (53, 54). Consequently, directly blocking the channel pore using Kir6.2-targeting antagonists, which represents a distinct action mechanism from that of sulfonylureas, might be an alternative strategy for treating these PNDM patients (35). The occurrence of side effects caused by off-target inhibition of the cardiac Kir6.2/SUR2A channel by these inhibitors could be further reduced as a previous study showed that this channel is at rest in normal physiological conditions (55). Recently, several protein inhibitors for the Kir6.2/SUR1 channel were characterized, including SpTx-1, SsTx, SsdTx1-3, and SsTx-4 in the present study (40, 41). Among them, the last five toxins belong to the same family because of their extremely high sequence homology, while SpTx-1 only has approximately 41% similarity to them. We showed that SsTx-4 inhibited the currents of the Kir6.2/SUR1 channel carrying several PNDM mutations with nanomolar affinity as its inhibition on the WT channel (Fig. S3, *A* and *B*). Moreover, SsTx-4 did not remarkably affect the currents of $Na_V1.4$ and $Na_V1.5$ channels (Fig. S3*C*), which are strongly involved in the *in vivo* toxicity of peptide toxins. We also showed that 5 μM SsTx-4 only slightly inhibited the currents of $Ca_V1.2$-1.3, $Ca_V2.1$-2.2, and $Ca_V3.1$-3.3 channels (Fig. S3*D*). SsTx was previously characterized as an antagonist of KCNQ and $K_V1.3$ channels, with the key residues in toxin being R12 and K13 for KCNQ, K11, R12, and K13 for $K_V1.3$, respectively (42, 56). We speculated SsTx-4 can inhibit KCNQ and $K_V1.3$ channels as well. Interestingly, K13 was also identified as the key molecular determinant in SsTx-4 for interacting with Kir1.1, Kir4.1, and Kir6.2/SUR1 channels, suggesting that this family of toxins used this common K to act on the K_V and Kir channels. However, whether K13 serves as the pore-blocking residue competing the K^+-binding site in the pore remains to be elucidated. As K11A and R12A mutations in SsTx-4 did not affect its inhibition on the Kir6.2/SUR1 channel, K11A, P15A, and Y16A mutations increased toxin's selectivity to Kir6.2/SUR1 against Kir1.1 and F43A mutation increased toxin's selectivity to Kir6.2/SUR1 against Kir4.1; it could be reasonably speculated that combining K11A, R12A, P15A, Y16A and F43A mutations in SsTx-4 would greatly reduce its $K_V1.3$, KCNQ, Kir1.1, and Kir4.1 activity to engineer a specific Kir6.2/SUR1 channel antagonist. The R12A and Y49A mutations increased toxin's activity on Kir4.1 channel by approximately 5- and 2-fold, respectively. It is possible to engineer an even more potent Kir4.1 antagonist than SsTx-4/R12A by combining these two mutations, given they worked synergistically. These speculations need to be experimentally tested in future studies.

The K_{ATP} channel is involved in adaption of the heart to stress during exercise as revealed by the study using global Kir6.2 KO mice (57). However, the KO strategy might bring some unexpected effects that could complicate the interpretation of the results. Therefore, specific Kir6.2 antagonists such as SsTx-4/R12A could be used as a pharmacological tool to explore the function of cardiac Kir6.2/SUR1 and Kir6.2/SUR2A channels without affecting the cardiac KNCQ channels. Moreover, the toxin SsTx-4/R12A could be useful in resolving the dispute whether or not SsTx-4 exhibits its lethal toxicity by blocking the KCNQ channels or the Kir6.2/SUR1 channel (41, 42), as it should have greatly reduced KNCQ activity but intact Kir6.2/SUR1 activity. Although the activity of SsTx and SsdTx1-3 on Kir1.1 and Kir4.1 channels was never reported, we speculated they are also potent Kir1.1 and Kir4.1 antagonist as SsTx-4. These toxins, especially the SsTx-4/R12A mutant with greatly improved Kir4.1 activity, could be used as pharmacological agents to assess the value of Kir4.1 channel as a drug target for treating depression, as a genetic study has revealed the critical role of Kir4.1 in the development of depression, but its nonselective antagonists such as quinacrine and sertraline showed no antidepressant effect in chronic social defeat stress-susceptible mice (20, 58).

We also tried to clarify the interacting residue pairs in the interface of SsTx-4 and Kir6.2 using thermodynamic mutant cycle analysis (59). As M137 is the only identified key residue in Kir6.2, we tested the possible coupling between M137 and the key residues in SsTx-4, including K13, F14, F44, F43/F44, K4/K45, K40/K45, and K4/K40/K45. However, no energetic coupling between them were observed. We could not exclude the involvement of other key residues in toxin and the channel as well, as the toxin residues are currently not thoroughly mutated and 15 of a total of 29 mutants with pore residue mutation are not functionally expressed in HEK293T cells, which precludes us from evaluating their role in toxin–channel association. Another possibility is that multiple interaction sites helped stabilize the toxin–channel complex. The redundancy of the key K and F residues in toxin's ββ sheet face and P-P loop region (K13, F14, K4, K40, K45, F43 and F44) also suggests the possibility of a dynamic and alternative interaction between SsTx-4 and Kir6.2. Molecular docking and molecular dynamic simulations would help illustrate the actual "pose" of toxin–channel interaction.

Experimental procedures

Venom and toxin purification

Centipede venom was collected by an electrical stimulation method, lyophilized, and stored at −80 °C. The venom powder was dissolved in ddH_2O to a final concentration of 5 mg/ml and subjected to RP-HPLC purification in a C18 column (10 × 250 mm, 5 μm, Welch Materials Inc) using a 50-min linear acetonitrile gradient from 10% to 60% at the flow rate of 3 ml/min. The fraction with Kir6.2/SUR1 inhibitory activity was further purified to homogeneity by two sequential activity–guided HPLC purifications: first by an RP-HPLC purification in an analytical C18 column (4.6 × 250 mm, 5 μm, Welch Materials Inc) using a 32-min linear acetonitrile gradient from 20% to 36% at the flow rate of 1 ml/min and then by a cation-exchange chromatography in a sulfonic acid–based cation exchange column (4.6 × 250 mm, 5 μm, Welch Materials Inc). The collected fraction was then desalted by another round of RP-HPLC purification. Combinatorial use of Edman

degradation and 5′-RACE had determined the full sequence of the toxin. The identity of the toxin was also cross-checked by matching its molecular weight (MW) determined by electrospray ionization MS with the theoretical MW. This toxin was named as SsTx-4.

Plasmids and site-directed mutation

The cDNAs encoding the *Homo sapiens* Kir subunits were subcloned in the eukaryotic expression vector pCMV-cHA (Kir2.2–2.4) or pcDNA3.1 (Kir1.1, Kir2.1, Kir4.1–4.2, Kir6.2, and Kir7.1). The SUR1 cDNA was a kind gift from professor Shibin Yang (Institute of Biomedical Sciences, Academia Sinica, Taipei, China) and subcloned in the vector pcDNA3 (60). SsTx-4's cDNA with an artificially added enterokinase (EK), and TEV protease recognition sequence at its 5′ end was optimized for recombinant expression in *E. coli* BL21(DE3), synthesized by GenScript (GenScript Corp), and cloned between the KpnI and BamHI sites in pET-32a(+) (pET-32a-EK/TEV-SsTx-4). The Kir6.2 truncant with its C-terminal 26 residues deleted, Kir6.2/ΔC26, was constructed by introducing a stop codon between A364 and R365 (hKir6.2 protein numbering) using site-directed mutagenesis. Other toxin and channel mutants were made by site-directed mutagenesis as well. Briefly, the parental channel or toxin plasmid was amplified by a pair of oppositely directed mutation primers with a 15-bp overlap using the KOD FX PCR kit (Toyobo Co, Ltd), then the product was treated with DpnI (Thermo Fisher Scientific) to remove the template DNA, and 10-μl digestion mix was directly used to transform 100-μl DH5α chemical competent cells. Plasmids from several transformants were extracted and sequenced to confirm that appropriate mutants were made.

Recombinant production of SsTx-4 and its mutants in E. coli

SsTx-4 and its mutants were produced as fusion proteins containing thioredoxin, 6×His tag, EK, and TEV proteases recognition sites at their N termini (thioredoxin-6×His-EK-TEV-toxin; the inducement conditions were: 37 °C, 0.1 mM IPTG, 12 h). After regular Ni bead purification, the fusion proteins were subjected to TEV digestion (Beijing Solarbio Science & Technology Co, Ltd; 16 °C for 6 h) to release the toxins, which were then purified to homogeneity by RP-HPLC.

Cell culture and transfection

HEK293T cells were maintained in Dulbecco's modified Eagle's medium (GIBCO) supplemented with 10% fetal bovine serum (GIBCO) and cultured in standard conditions (37 °C, 5% CO_2, saturated humidity). Transfection was performed when the cell confluence reached 70% to 90%. The plasmid for each Kir channel was cotransfected with pEGFP-N1 plasmid into HEK293T cells using Lipofectamine 2000 following the manufacturer's instructions (Invitrogen Corporation). For the Kir6.2/SUR1 channel, Kir6.2, SUR1 and pEGFP-N1 plasmids were cotransfected. Four to six hours after transfection, cells were seeded onto poly-lysine (PLL)-coated coverslips, and 24 h later, the positively transfected cells as indicated by green fluorescence were randomly selected for patch-clamp analysis.

Electrophysiology

Whole-cell patch clamp recordings were performed in an EPC10 patch-clamp platform (HEKA Elektronik). The capillary pipettes were prepared in a PC-10 puller (NARISHIGE) using a two-step program. Only the pipette tip was filled with the pipette solution to minimize the capacitance, and the artificial capacitance effect was canceled by sequential fast and slow capacitance compensation using the computer-controlled circuit of the amplifier. The series resistance after establishing the whole-cell configuration should be less than 10 MΩ, and 80% series resistance compensation was used (speed value = 100 μs), which effectively reduced the voltage error during the recording. Moreover, to minimize the contamination of Kir currents by the leak currents, cells with seal resistance lower than GΩ after break-in were discarded. The bath solution for recording the currents of Kir1.1 and its mutant, Kir2.1 to 2.4, Kir4.1 and its mutant, Kir4.2 and Kir7.1 contains (in mM) 120 NaCl, 5 KCl, 1.5 $CaCl_2$, 1 $MgCl_2$, 10 glucose, and 10 Hepes (adjusting the pH to 7.4 with NaOH). The corresponding pipette solution contains (in mM) 140 KCl, 2 $MgCl_2$, 0.1 EGTA, 4 Na-ATP, and 10 Hepes (adjusting the pH to 7.3 with KOH). The bath solution for recording the currents of Kir6.2 and its mutants contains (in mM) 150 NaCl, 5 KCl, 2 $CaCl_2$, 1 $MgCl_2$, and 10 Hepes (adjusting the pH to 7.2 with NaOH). The pipette solution contains (in mM) 135 K-gluconate, 15 KCl, 0.5 Na-ATP, 0.05 EGTA, 10 Na-phosphocreatine, and 10 Hepes (adjusting the pH to 7.2 with KOH). All chemicals were from Sigma-Aldrich. Cells were held at −70 mV, and Kir currents were elicited by a 100-ms step hyperpolarization to −140 mV (−90 mV for Kir2.1–2.4 channels, which have much stronger inward rectification) followed by a 100-ms depolarization to −40 mV. Currents were low-pass filtered at 2.9 kHz cutoff frequency and sampled at 50 kHz using the PATCHMASTER software (HEKA Elektronik). Data were analyzed using Igor Pro 6.10A (WaveMetrics, Inc), Origin 8 (OriginLab Corp), SigmaPlot 10.0 (SYSTAT Software, Inc), and GraphPad Prism 5.01 (GraphPad Software, Inc). The current inhibition of Kirs after SsTx-4 application was complete within one sweep interval (5 s), thus the time constant of toxin associating with the channel (τ_{on}) could not be precisely estimated. However, the current recovery of Kirs upon washing off the toxin was relatively slow and the time course was fitted by the equation: $y = y_{(0)} + a\ (1 - e^{-x/\tau})$, in which τ represents the time constant for toxin dissociating from the channel. The dose–response curves for SsTx-4-inhibiting Kir channels were fitted by the Hill logistic equation to estimate the IC_{50}. In Figure 4, we treated the channel with a single dose of toxin to reach an approximately 40% to 60% current inhibition (except for testing the inhibition of mutant toxins SsTx-4/K13A, SsTx-4/F43A, SsTx-4/F44A, and SsTx-4/F43A/F44A on the Kir4.1 channel, in which 10 μM toxin treatment only caused approximately 10%–25% current inhibition), and the IC_{50} value was determined by the following equation: IC_{50}=

$[Tx] \times I_{res}/(1 - I_{res})$, in which [Tx] and I_{res} represent the toxin concentration and the proportion of residual current after toxin treatment, respectively.

Data analysis

Data were presented as the mean ± SD, n represents the number of separate experimental cells. Statistical significance was assessed using paired *t* test or one-way ANOVA, comparison between multiple groups was performed using post hoc analysis with the Dunnett's method, and statistical significance was accepted at $p < 0.05$.

Data availability

All of the data are in the article.

Supporting information—This article contains supporting information.

Acknowledgments—This work was supported by the National Natural Science Foundation of China (Grant Nos. 31600669, 32071262, 31770832, and 31872718), the Science and Technology Innovation Program of Hunan Province (2020RC4023), the Natural Science Foundation of Hunan Province (Grant No. 2018JJ3339), and the Research Foundation of the Education Department of Hunan Province (Grant No. 18B015). We thank Professor Shibin Yang (Institute of Biomedical Sciences, Academia Sinica, Taipei, China) for providing us with the SUR1 cDNA.

Author contributions—D. T., J. X., Y. L., P. Z., X. K., and C. T. data curation; D. T., J. X., Y. L., P. Z., H. H., and C. T. investigation; D. T. and J. X. project administration; H. H. software; S. L., C. T., and Z. L. supervision; S. L., C. T., and Z. L. funding acquisition; C. T. and Z. L. conceptualization; C. T. and Z. L. methodology; C. T. and Z. L. writing–original draft.

Conflict of interest—The authors declare that they have no conflicts of interest with the contents of this article.

Abbreviations—The abbreviations used are: EK, enterokinase; Kirs, inwardly rectifying potassium channels; MW, molecular weight; PNDM, permanent neonatal diabetes mellitus; SF, selectivity filter; SUR, sulfonylurea receptor.

References

1. Sansom, M. S., Shrivastava, I. H., Bright, J. N., Tate, J., Capener, C. E., and Biggin, P. C. (2002) Potassium channels: Structures, models, simulations. *Biochim. Biophys. Acta* **1565**, 294–307
2. Hibino, H., Inanobe, A., Furutani, K., Murakami, S., Findlay, I., and Kurachi, Y. (2010) Inwardly rectifying potassium channels: Their structure, function, and physiological roles. *Physiol. Rev.* **90**, 291–366
3. Doupnik, C. A., Davidson, N., and Lester, H. A. (1995) The inward rectifier potassium channel family. *Curr. Opin. Neurobiol.* **5**, 268–277
4. Bichet, D., Haass, F. A., and Jan, L. Y. (2003) Merging functional studies with structures of inward-rectifier K(+) channels. *Nat. Rev. Neurosci.* **4**, 957–967
5. Heginbotham, L., Lu, Z., Abramson, T., and MacKinnon, R. (1994) Mutations in the K+ channel signature sequence. *Biophys. J.* **66**, 1061–1067
6. Clement, J. P.t., Kunjilwar, K., Gonzalez, G., Schwanstecher, M., Panten, U., Aguilar-Bryan, L., and Bryan, J. (1997) Association and stoichiometry of K(ATP) channel subunits. *Neuron* **18**, 827–838
7. Gribble, F. M., Tucker, S. J., and Ashcroft, F. M. (1997) The essential role of the Walker A motifs of SUR1 in K-ATP channel activation by Mg-ADP and diazoxide. *EMBO J.* **16**, 1145–1152
8. Inagaki, N., Gonoi, T., Clement, J. P., Wang, C. Z., Aguilar-Bryan, L., Bryan, J., and Seino, S. (1996) A family of sulfonylurea receptors determines the pharmacological properties of ATP-sensitive K+ channels. *Neuron* **16**, 1011–1017
9. Isomoto, S., Kondo, C., Yamada, M., Matsumoto, S., Higashiguchi, O., Horio, Y., Matsuzawa, Y., and Kurachi, Y. (1996) A novel sulfonylurea receptor forms with BIR (Kir6.2) a smooth muscle type ATP-sensitive K+ channel. *J. Biol. Chem.* **271**, 24321–24324
10. Yamada, M., Isomoto, S., Matsumoto, S., Kondo, C., Shindo, T., Horio, Y., and Kurachi, Y. (1997) Sulphonylurea receptor 2B and Kir6.1 form a sulphonylurea-sensitive but ATP-insensitive K+ channel. *J. Physiol.* **499**, 715–720
11. Ashcroft, F. M., and Rorsman, P. (2013) K(ATP) channels and islet hormone secretion: New insights and controversies. *Nat. Rev. Endocrinol.* **9**, 660–669
12. Bao, L., Kefaloyianni, E., Lader, J., Hong, M., Morley, G., Fishman, G. I., Sobie, E. A., and Coetzee, W. A. (2011) Unique properties of the ATP-sensitive K(+) channel in the mouse ventricular cardiac conduction system. *Circ. Arrhythm Electrophysiol.* **4**, 926–935
13. Aziz, Q., Thomas, A. M., Gomes, J., Ang, R., Sones, W. R., Li, Y., Ng, K. E., Gee, L., and Tinker, A. (2014) The ATP-sensitive potassium channel subunit, Kir6.1, in vascular smooth muscle plays a major role in blood pressure control. *Hypertension* **64**, 523–529
14. Tinker, A., Aziz, Q., Li, Y., and Specterman, M. (2018) ATP-sensitive potassium channels and their physiological and pathophysiological roles. *Compr. Physiol.* **8**, 1463–1511
15. Nichols, C. G., and Lee, S. J. (2018) Polyamines and potassium channels: A 25-year romance. *J. Biol. Chem.* **293**, 18779–18788
16. Baronas, V. A., and Kurata, H. T. (2014) Inward rectifiers and their regulation by endogenous polyamines. *Front. Physiol.* **5**, 325
17. Priest, B. T., and Pasternak, A. (2017) The therapeutic potential of targeting the Kir1.1 (renal outer medullary K(+)) channel. *Future Med. Chem.* **9**, 1963–1977
18. Elfert, K. A., Geller, D. S., Nelson-Williams, C., Lifton, R. P., Al-Malki, H., and Nauman, A. (2020) Late-Onset Bartter syndrome type II due to a homozygous mutation in KCNJ1 gene: A case report and literature review. *Am. J. Case Rep.* **21**, e924527
19. Ji, W., Foo, J. N., O'Roak, B. J., Zhao, H., Larson, M. G., Simon, D. B., Newton-Cheh, C., State, M. W., Levy, D., and Lifton, R. P. (2008) Rare independent mutations in renal salt handling genes contribute to blood pressure variation. *Nat. Genet.* **40**, 592–599
20. Cui, Y., Yang, Y., Ni, Z., Dong, Y., Cai, G., Foncelle, A., Ma, S., Sang, K., Tang, S., Li, Y., Shen, Y., Berry, H., Wu, S., and Hu, H. (2018) Astroglial Kir4.1 in the lateral habenula drives neuronal bursts in depression. *Nature* **554**, 323–327
21. O'Hare, J. P., Hanif, W., Millar-Jones, D., Bain, S., Hicks, D., Leslie, R. D., and Barnett, A. H. (2015) NICE guidelines for type 2 diabetes: Revised but still not fit for purpose. *Diabet. Med.* **32**, 1398–1403
22. Yan, F. F., Lin, Y. W., MacMullen, C., Ganguly, A., Stanley, C. A., and Shyng, S. L. (2007) Congenital hyperinsulinism associated ABCC8 mutations that cause defective trafficking of ATP-sensitive K+ channels: Identification and rescue. *Diabetes* **56**, 2339–2348
23. Taneja, T. K., Mankouri, J., Karnik, R., Kannan, S., Smith, A. J., Munsey, T., Christesen, H. B., Beech, D. J., and Sivaprasadarao, A. (2009) Sar1-GTPase-dependent ER exit of KATP channels revealed by a mutation causing congenital hyperinsulinism. *Hum. Mol. Genet.* **18**, 2400–2413
24. Hattersley, A. T., and Ashcroft, F. M. (2005) Activating mutations in Kir6.2 and neonatal diabetes: New clinical syndromes, new scientific insights, and new therapy. *Diabetes* **54**, 2503–2513
25. Bonfanti, D. H., Alcazar, L. P., Arakaki, P. A., Martins, L. T., Agustini, B. C., de Moraes Rego, F. G., and Frigeri, H. R. (2015) ATP-dependent potassium channels and type 2 diabetes mellitus. *Clin. Biochem.* **48**, 476–482
26. Rorsman, P., and Ashcroft, F. M. (2018) Pancreatic beta-cell electrical activity and insulin secretion: Of mice and men. *Physiol. Rev.* **98**, 117–214

27. Swale, D. R., Kharade, S. V., and Denton, J. S. (2014) Cardiac and renal inward rectifier potassium channel pharmacology: Emerging tools for integrative physiology and therapeutics. *Curr. Opin. Pharmacol.* **15**, 7–15
28. Rodriguez-Menchaca, A. A., Navarro-Polanco, R. A., Ferrer-Villada, T., Rupp, J., Sachse, F. B., Tristani-Firouzi, M., and Sanchez-Chapula, J. A. (2008) The molecular basis of chloroquine block of the inward rectifier Kir2.1 channel. *Proc. Natl. Acad. Sci. U. S. A.* **105**, 1364–1368
29. Bhave, G., Chauder, B. A., Liu, W., Dawson, E. S., Kadakia, R., Nguyen, T. T., Lewis, L. M., Meiler, J., Weaver, C. D., Satlin, L. M., Lindsley, C. W., and Denton, J. S. (2011) Development of a selective small-molecule inhibitor of Kir1.1, the renal outer medullary potassium channel. *Mol. Pharmacol.* **79**, 42–50
30. Rodriguez-Menchaca, A. A., Arechiga-Figueroa, I. A., and Sanchez-Chapula, J. A. (2016) The molecular basis of chloroethylclonidine block of inward rectifier (Kir2.1 and Kir4.1) K(+) channels. *Pharmacol. Rep.* **68**, 383–389
31. Moran-Zendejas, R., Delgado-Ramirez, M., Xu, J., Valdes-Abadia, B., Arechiga-Figueroa, I. A., Cui, M., and Rodriguez-Menchaca, A. A. (2020) *In vitro* and in silico characterization of the inhibition of Kir4.1 channels by aminoglycoside antibiotics. *Br. J. Pharmacol.* **177**, 4548–4560
32. Doupnik, C. A. (2017) Venom-derived peptides inhibiting Kir channels: Past, present, and future. *Neuropharmacology* **127**, 161–172
33. Arechiga-Figueroa, I. A., Marmolejo-Murillo, L. G., Cui, M., Delgado-Ramirez, M., van der Heyden, M. A. G., Sanchez-Chapula, J. A., and Rodriguez-Menchaca, A. A. (2017) High-potency block of Kir4.1 channels by pentamidine: Molecular basis. *Eur. J. Pharmacol.* **815**, 56–63
34. Imredy, J. P., Chen, C., and MacKinnon, R. (1998) A snake toxin inhibitor of inward rectifier potassium channel ROMK1. *Biochemistry* **37**, 14867–14874
35. Jin, W., and Lu, Z. (1998) A novel high-affinity inhibitor for inward-rectifier K+ channels. *Biochemistry* **37**, 13291–13299
36. Lu, Z., and MacKinnon, R. (1997) Purification, characterization, and synthesis of an inward-rectifier K+ channel inhibitor from scorpion venom. *Biochemistry* **36**, 6936–6940
37. Jin, W., Klem, A. M., Lewis, J. H., and Lu, Z. (1999) Mechanisms of inward-rectifier K+ channel inhibition by tertiapin-Q. *Biochemistry* **38**, 14294–14301
38. Hu, J., Qiu, S., Yang, F., Cao, Z., Li, W., and Wu, Y. (2013) Unique mechanism of the interaction between honey bee toxin TPNQ and rKir1.1 potassium channel explored by computational simulations: Insights into the relative insensitivity of channel towards animal toxins. *PLoS One* **8**, e67213
39. Ramu, Y., Klem, A. M., and Lu, Z. (2001) Titration of tertiapin-Q inhibition of ROMK1 channels by extracellular protons. *Biochemistry* **40**, 3601–3605
40. Ramu, Y., Xu, Y., and Lu, Z. (2018) A novel high-affinity inhibitor against the human ATP-sensitive Kir6.2 channel. *J. Gen. Physiol.* **150**, 969–976
41. Ramu, Y., and Lu, Z. (2019) A family of orthologous proteins from centipede venoms inhibit the hKir6.2 channel. *Sci. Rep.* **9**, 14088
42. Luo, L., Li, B., Wang, S., Wu, F., Wang, X., Liang, P., Ombati, R., Chen, J., Lu, X., Cui, J., Lu, Q., Zhang, L., Zhou, M., Tian, C., Yang, S., *et al.* (2018) Centipedes subdue giant prey by blocking KCNQ channels. *Proc. Natl. Acad. Sci. U. S. A.* **115**, 1646–1651
43. Goldstein, S. A., and Miller, C. (1993) Mechanism of charybdotoxin block of a voltage-gated K+ channel. *Biophys. J.* **65**, 1613–1619
44. MacKinnon, R., Heginbotham, L., and Abramson, T. (1990) Mapping the receptor site for charybdotoxin, a pore-blocking potassium channel inhibitor. *Neuron* **5**, 767–771
45. Goldstein, S. A., and Miller, C. (1992) A point mutation in a Shaker K+ channel changes its charybdotoxin binding site from low to high affinity. *Biophys. J.* **62**, 5–7
46. Kharade, S. V., Kurata, H., Bender, A. M., Blobaum, A. L., Figueroa, E. E., Duran, A., Kramer, M., Days, E., Vinson, P., Flores, D., Satlin, L. M., Meiler, J., Weaver, C. D., Lindsley, C. W., Hopkins, C. R., *et al.* (2018) Discovery, characterization, and effects on renal fluid and electrolyte excretion of the Kir4.1 potassium channel pore blocker, VU0134992. *Mol. Pharmacol.* **94**, 926–937
47. Tucker, S. J., Gribble, F. M., Zhao, C., Trapp, S., and Ashcroft, F. M. (1997) Truncation of Kir6.2 produces ATP-sensitive K+ channels in the absence of the sulphonylurea receptor. *Nature* **387**, 179–183
48. Luna-Ramirez, K., Csoti, A., McArthur, J. R., Chin, Y. K. Y., Anangi, R., Najera, R. D. C., Possani, L. D., King, G. F., Panyi, G., Yu, H., Adams, D. J., and Finol-Urdaneta, R. K. (2020) Structural basis of the potency and selectivity of urotoxin, a potent Kv1 blocker from scorpion venom. *Biochem. Pharmacol.* **174**, 113782
49. Dauplais, M., Lecoq, A., Song, J., Cotton, J., Jamin, N., Gilquin, B., Roumestand, C., Vita, C., de Medeiros, C. L., Rowan, E. G., Harvey, A. L., and Menez, A. (1997) On the convergent evolution of animal toxins. Conservation of a diad of functional residues in potassium channel-blocking toxins with unrelated structures. *J. Biol. Chem.* **272**, 4302–4309
50. Gloyn, A. L., Pearson, E. R., Antcliff, J. F., Proks, P., Bruining, G. J., Slingerland, A. S., Howard, N., Srinivasan, S., Silva, J. M., Molnes, J., Edghill, E. L., Frayling, T. M., Temple, I. K., Mackay, D., Shield, J. P., *et al.* (2004) Activating mutations in the gene encoding the ATP-sensitive potassium-channel subunit Kir6.2 and permanent neonatal diabetes. *N. Engl. J. Med.* **350**, 1838–1849
51. Vaxillaire, M., Populaire, C., Busiah, K., Cave, H., Gloyn, A. L., Hattersley, A. T., Czernichow, P., Froguel, P., and Polak, M. (2004) Kir6.2 mutations are a common cause of permanent neonatal diabetes in a large cohort of French patients. *Diabetes* **53**, 2719–2722
52. Babenko, A. P., Polak, M., Cave, H., Busiah, K., Czernichow, P., Scharfmann, R., Bryan, J., Aguilar-Bryan, L., Vaxillaire, M., and Froguel, P. (2006) Activating mutations in the ABCC8 gene in neonatal diabetes mellitus. *N. Engl. J. Med.* **355**, 456–466
53. Remedi, M. S., Kurata, H. T., Scott, A., Wunderlich, F. T., Rother, E., Kleinridders, A., Tong, A., Bruning, J. C., Koster, J. C., and Nichols, C. G. (2009) Secondary consequences of beta cell inexcitability: Identification and prevention in a murine model of K(ATP)-induced neonatal diabetes mellitus. *Cell Metab.* **9**, 140–151
54. Proks, P., de Wet, H., and Ashcroft, F. M. (2013) Molecular mechanism of sulphonylurea block of K(ATP) channels carrying mutations that impair ATP inhibition and cause neonatal diabetes. *Diabetes* **62**, 3909–3919
55. Zhang, H., Flagg, T. P., and Nichols, C. G. (2010) Cardiac sarcolemmal K(ATP) channels: Latest twists in a questing tale! *J. Mol. Cell. Cardiol.* **48**, 71–75
56. Du, C., Li, J., Shao, Z., Mwangi, J., Xu, R., Tian, H., Mo, G., Lai, R., and Yang, S. (2019) Centipede KCNQ inhibitor SsTx also targets KV1.3. *Toxins (Basel)* **11**, 76
57. Zingman, L. V., Hodgson, D. M., Bast, P. H., Kane, G. C., Perez-Terzic, C., Gumina, R. J., Pucar, D., Bienengraeber, M., Dzeja, P. P., Miki, T., Seino, S., Alekseev, A. E., and Terzic, A. (2002) Kir6.2 is required for adaptation to stress. *Proc. Natl. Acad. Sci. U. S. A.* **99**, 13278–13283
58. Xiong, Z., Zhang, K., Ishima, T., Ren, Q., Ma, M., Pu, Y., Chang, L., Chen, J., and Hashimoto, K. (2019) Lack of rapid antidepressant effects of Kir4.1 channel inhibitors in a chronic social defeat stress model: Comparison with (R)-ketamine. *Pharmacol. Biochem. Behav.* **176**, 57–62
59. Jin, W., and Lu, Z. (1999) Synthesis of a stable form of tertiapin: A high-affinity inhibitor for inward-rectifier K+ channels. *Biochemistry* **38**, 14286–14293
60. Yang, Y. Y., Long, R. K., Ferrara, C. T., Gitelman, S. E., German, M. S., and Yang, S. B. (2017) A new familial form of a late-onset, persistent hyperinsulinemic hypoglycemia of infancy caused by a novel mutation in KCNJ11. *Channels (Austin)* **11**, 636–647